

CONFIDENTIAL

Copy
RM 1531186

NACA RM 153118b

NACA

RESEARCH MEMORANDUM

SOME EFFECTS OF AEROELASTICITY AND SWEEPBACK ON THE
ROLLING EFFECTIVENESS AND DRAG OF A 1/11-SCALE
MODEL OF THE BELL X-5 AIRPLANE WING AT
MACH NUMBERS FROM 0.6 TO 1.5

By Roland D. English

CLASSIFICATION ~~CANCELLED~~ Langley Aeronautical Laboratory
Langley Field, Va.

Authority NACA RM 153118b Date 12/14/53

RN 700.94

By 4277 1/18/56 See _____

LANGLEY AERONAUTICAL LABORATORY
LANGLEY FIELD, VIRGINIA

CLASSIFIED DOCUMENT

This material contains information affecting the National Defense of the United States within the meaning of the espionage laws, Title 18, U.S.C., Secs. 793 and 794, the transmission or revelation of which in any manner to an unauthorized person is prohibited by law.

NATIONAL ADVISORY COMMITTEE
FOR AERONAUTICS

WASHINGTON

November 18, 1953

CONFIDENTIAL



NATIONAL ADVISORY COMMITTEE FOR AERONAUTICS

RESEARCH MEMORANDUM

SOME EFFECTS OF AEROELASTICITY AND SWEEPBACK ON THE
ROLLING EFFECTIVENESS AND DRAG OF A 1/11-SCALE
MODEL OF THE BELL X-5 AIRPLANE WING AT
MACH NUMBERS FROM 0.6 TO 1.5

By Roland D. English

SUMMARY


The Langley Pilotless Aircraft Research Division has made an investigation to determine some effects of aeroelasticity and sweepback on the rolling effectiveness and drag of a 1/11-scale model of the variable-sweep Bell X-5 airplane wing at zero angle of attack and zero angle of sideslip. The investigation was made by means of rocket-powered models in free flight. Rolling effectiveness and drag data were obtained over a range of Mach number from 0.6 to 1.5.

Results of the investigation indicate that the Bell X-5 airplane with present wing construction is subject to severe rolling effectiveness losses due to wing flexibility.

Increasing the angle of wing sweepback increases the rolling effectiveness in the Mach number range above 0.65. Increasing the angle of sweepback also decreases the subsonic drag coefficient and increases the Mach number at which transonic drag rise occurs.

INTRODUCTION

The Langley Pilotless Aircraft Research Division has made an investigation to determine some effects of aeroelasticity and sweepback on the steady-state rolling effectiveness and drag of a 1/11-scale model of the variable-sweep Bell X-5 airplane wing. The tests were made by means of rocket-propelled models in free flight at zero angle of attack and zero angle of sideslip over a Mach number range from 0.6 to 1.5.



Rolling effectiveness and drag data were obtained for wings of two stiffnesses at both 20° and 46.5° sweepback. Results of the present investigation are compared with data obtained from flight tests of the full-scale airplane with the wings swept back 20° .

SYMBOLS

b	diameter of circle spanned by wing tips at 38 percent chord, ft
c	local wing chord, ft
C_D	drag coefficient based on exposed area of two wing panels having the 38-percent-chord line unswept (1.110 sq ft)
h	altitude, ft
M	Mach number
m	static twisting couple applied near wing tip in a plane normal to 38-percent-chord line and normal to wing chord plane, in-lb
P	total static bending load distributed along the 38-percent-chord line of one wing, lb
p	rolling velocity, radians/sec
p_0	sea-level static pressure, lb/sq ft
p_a	static pressure at altitude, lb/sq ft
R	Reynolds number based on mean exposed chord of unswept wing panel (0.445 ft)
V	model flight-path velocity, ft/sec
$pb/2V$	wing tip helix angle, radians
α	angle of attack, deg
β	angle of sideslip, deg
θ	angle of twist in plane of and resulting from m, radians
δ	deflection of 38-percent-chord line resulting from P, in.

δ_a aileron deflection measured perpendicular to hinge line, deg
 Λ angle of sweepback of the quarter-chord line, deg
 θ/m torsional stiffness parameter, radians/in-lb
 δ/P flexural-stiffness parameter, in./lb

Subscripts:

T total deflection (absolute sum of right and left aileron deflections)

DESCRIPTION OF MODELS AND TESTS

The wings tested in this investigation were 1/11-scale models of the Bell X-5 airplane wing. The unswept Bell X-5 wing has an aspect ratio of 6.202, a taper ratio of 0.494, and an NACA 64A-series airfoil section perpendicular to the 38-percent-chord line. The maximum thickness is 0.11c at the root and 0.0828c at the tip. Rolling power is provided by a partial-span, plain, trailing-edge aileron (see figs. 1 and 2). In models 1 and 4 of the present tests, $b/2$ was 1.394 feet, the exposed wing area was 1.091 square feet, and the quarter-chord line was swept back 20° . In models 2 and 3, $b/2$ was 1.096 feet, the exposed wing area was 1.064 square feet, and the quarter-chord line was swept back 46.5° . Aileron deflection was 10° , measured perpendicular to the hinge line, for all models. Photographs of typical models are shown in figure 1. Figure 2 presents sketches showing geometric details and dimensions. All models had free-spinning tails as shown in figures 1 and 2.

Construction details of all wings are shown in the section views of figure 3. A stiff construction was used for models 2 and 4, whereas the wing construction of models 1 and 3 was selected so as to approximate the scaled-down stiffness characteristics of the full-scale Bell X-5 airplane wing. The variation along the span of the torsional-stiffness parameter θ/m was obtained for all models by applying a known static twisting couple near the wing tip and measuring the resulting angle of twist at various spanwise stations. The torsional-stiffness characteristics of all models are shown together with the scaled-down values for the Bell X-5 wing in figure 4. The flexural-stiffness parameter δ/P was obtained by distributing a load along the 38-percent-chord line and measuring the resulting deflection. The load distribution and resulting δ/P values are presented as a function of spanwise station in figure 5; also included in this figure is the spanwise variation of scaled-down δ/P values for the airplane wing.

Models 2 and 3 were propelled to a maximum Mach number of 1.5 by a two-stage rocket-propulsion system. A single booster rocket was used to propel models 1 and 4 to a Mach number of 0.9. Flight-path velocity, rolling velocity, and space coordinates were obtained continuously during a period of free flight following burnout of the last propulsion stage, by means of radio (spinsonde) and radar equipment. The previous data were used with atmospheric data from radiosondes to obtain the variation of the rolling effectiveness parameter $pb/2V$ and drag coefficient C_D with Mach number. The use of free-spinning tails kept all models at essentially zero angle of attack and zero angle of sideslip during the tests. The range of test Reynolds number is given as a function of Mach number in figure 6. A discussion of the test method is given in more detail in references 1 and 2.

ACCURACY

The inaccuracies resulting from construction tolerances and other limitations are estimated to be within the following limits:

	Subsonic	Supersonic
$pb/2V$	± 0.003	± 0.002
C_D	± 0.003	± 0.002
M	± 0.01	± 0.01

RESULTS AND DISCUSSION

The variation of p_a/p_o and the rolling effectiveness parameter $pb/2V$ with Mach number is shown in figure 7. These values of $pb/2V$ have been corrected by the method of reference 3 for the random wing incidence errors resulting from construction tolerances. No attempt was made to correct $pb/2V$ for inertia effects since reference 1 shows this correction to be negligible. Figure 7 shows that aeroelastic reversal occurred for both flexible-wing configurations. Since the flexible model wing closely approximates the scaled-down stiffness characteristics of the airplane wing, the Bell X-5 airplane with present wing construction is subject to severe rolling effectiveness losses due to wing flexibility at low altitudes. Calculations (using the method of ref. 4) indicate that the rolling effectiveness losses would be over 20 percent up to altitudes of about 35,000 feet. Changing the angle of sweepback from 20° to 46.5° increases the rolling effectiveness over the Mach number range above $M = 0.65$ and increases the Mach number at which aeroelastic reversal occurs.

Rigid wing rolling effectiveness values were calculated by the method of reference 4 using the stiff wing data in figure 7. The rigid wing values were used in turn to calculate flexible wing rolling effectiveness at the model flight altitudes. The variation of calculated rigid and flexible wing rolling effectiveness with Mach number is presented in figure 8. The data of figure 7 are repeated in figure 8 for purposes of comparison of calculated and experimental values.

The method of reference 4 was used also to calculate flexible-wing rolling effectiveness at an altitude of 25,000 feet for the 20° sweptback-wing configuration. This calculated rolling effectiveness is compared to that of the full-scale airplane at zero angle of sideslip in figure 9. The data for the airplane were collected at Edwards Air Force Base, Calif., and published in reference 5 for fixed control flight. The data for $\beta = 0^\circ$ were not published.

The variation of $\frac{p_b/2V}{\delta a_T}$ with Mach number is presented in figure 10 for the flexible model and the airplane with the wing swept back 20°. No data are available at present for the airplane with the wing swept back 46.5°.

The variation of drag coefficient C_D with Mach number is presented for all models in figure 11. Drag coefficient has been obtained for the body plus free-spinning tail and is included for reference. Figure 11 shows that subsonic drag coefficient is lower, and that transonic drag rise occurs at a higher Mach number, for the wing swept back 46.5° than for the one swept back 20°. Since the subsonic Reynolds numbers are in the region of transition from laminar to turbulent flow, the drag reduction is probably due in part to a difference in Reynolds numbers (see fig. 6). However, it is doubtful that difference in Reynolds numbers accounts for the total drag reduction, so it is believed that changing the angle of sweepback from 20° to 46.5° reduces the subsonic drag coefficient. No appreciable effect of wing flexibility on drag was found.

CONCLUSIONS

The results of an investigation of some effects of aeroelasticity and sweepback on the rolling effectiveness and drag of a 1/11-scale model of the Bell X-5 airplane wing-aileron configuration indicate the following:

1. The Bell X-5 airplane with present wing construction is subject to rolling effectiveness losses of over 20 percent due to wing flexibility at altitudes up to 35,000 feet.

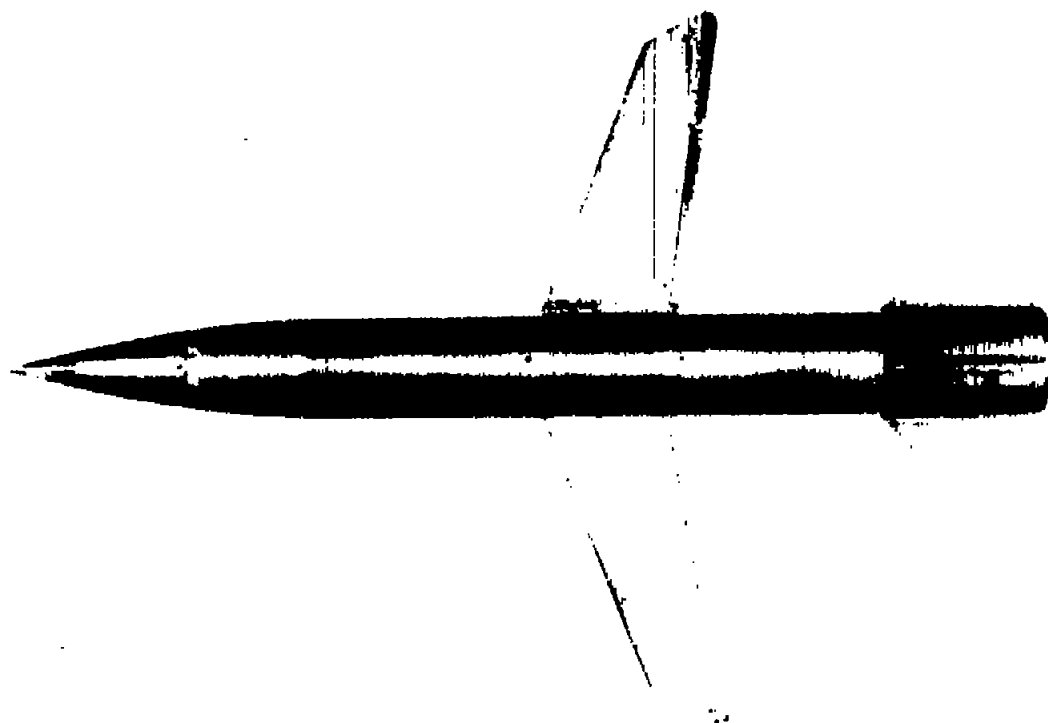
2. Changing the angle of wing sweepback from 20° to 46.5° increased the rolling effectiveness in the Mach number range above 0.65 and increased the Mach number at which aeroelastic reversal occurred.

3. No effects of wing flexibility on drag were found; increasing the angle of wing sweepback decreased the subsonic drag coefficient and increased the Mach number at which transonic drag rise occurs.

Langley Aeronautical Laboratory,
National Advisory Committee for Aeronautics,
Langley Field, Va., September 3, 1953.

REFERENCES

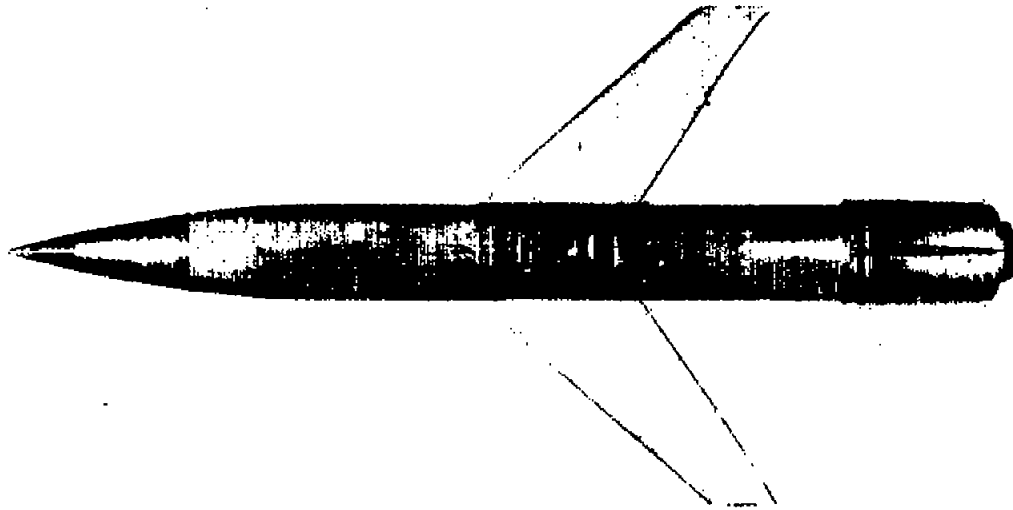
1. Sandahl, Carl A., and Marino, Alfred A.: Free-Flight Investigation of Control Effectiveness of Full-Span 0.2-Chord Plain Ailerons at High Subsonic, Transonic, and Supersonic Speeds To Determine Some Effects of Section Thickness and Wing Sweepback. NACA RM L7D02, 1947.
2. Pitkin, Marvin, Gardner, William N., and Gurfman, Howard J., Jr.: Results of Preliminary Flight Investigation of Aerodynamic Characteristics of the NACA Two-Stage Supersonic Research Model RM-1 Stabilized in Roll at Transonic and Supersonic Velocities. NACA RM L6J23, 1947.
3. Strass, H. Kurt, and Marley, Edward T.: Rolling Effectiveness of All-Movable Wings at Small Angles of Incidence at Mach Numbers From 0.6 to 1.6. NACA RM L51H03, 1951.
4. Strass, H. Kurt, and Stephens, Emily W.: An Engineering Method for the Determination of Aeroelastic Effects Upon the Rolling Effectiveness of Ailerons on Swept Wings. NACA RM L53H14, 1953.
5. Finch, Thomas W., and Briggs, Donald W.: Preliminary Results of Stability and Control Investigation of the Bell X-5 Research Airplane. NACA RM L52K18b, 1953.



(a) Model 1.

L-74986.1.

Figure 1.- Photographs of typical test models.



(b) Model 3.

L-74985.1

Figure 1.- Concluded.

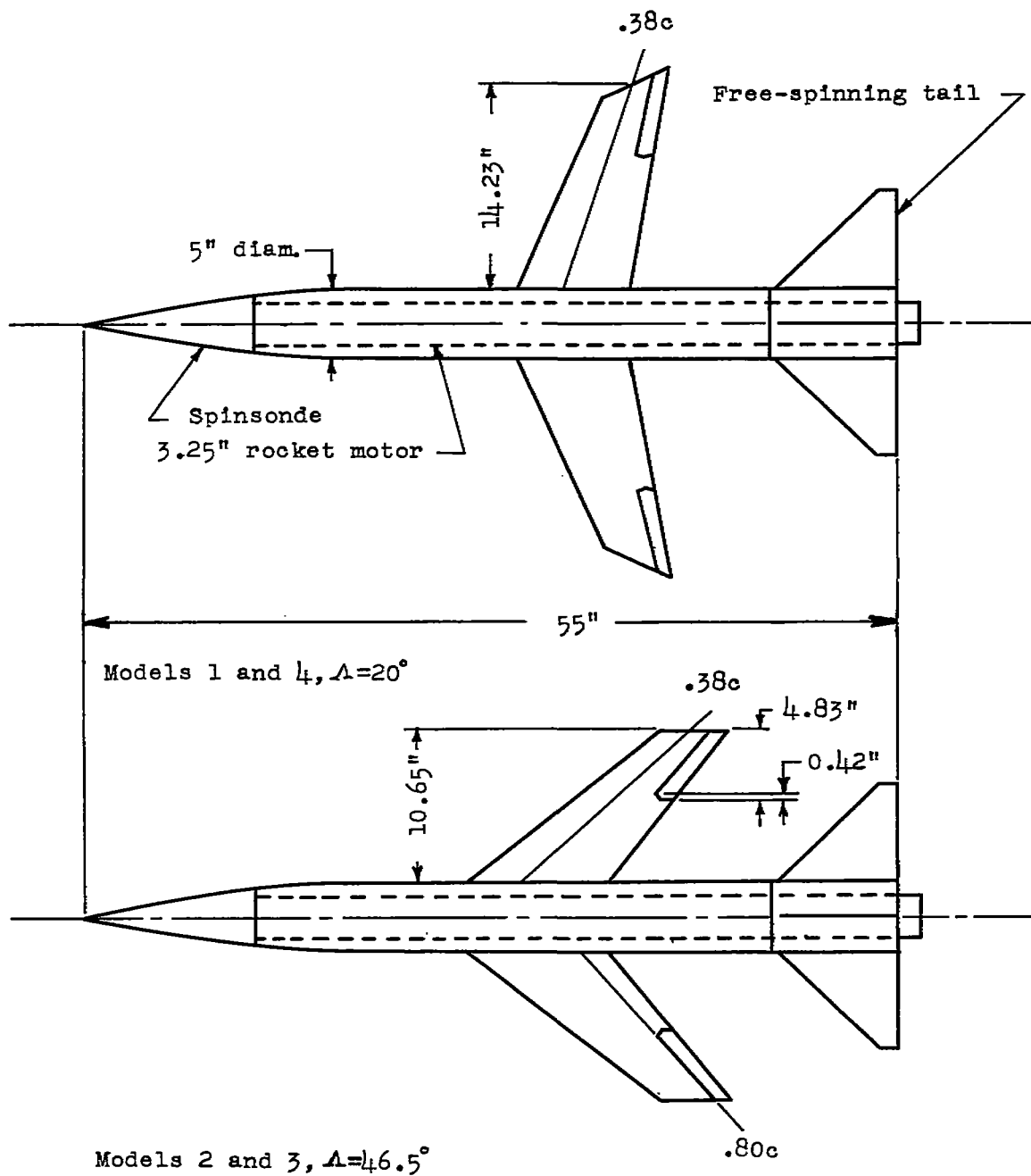
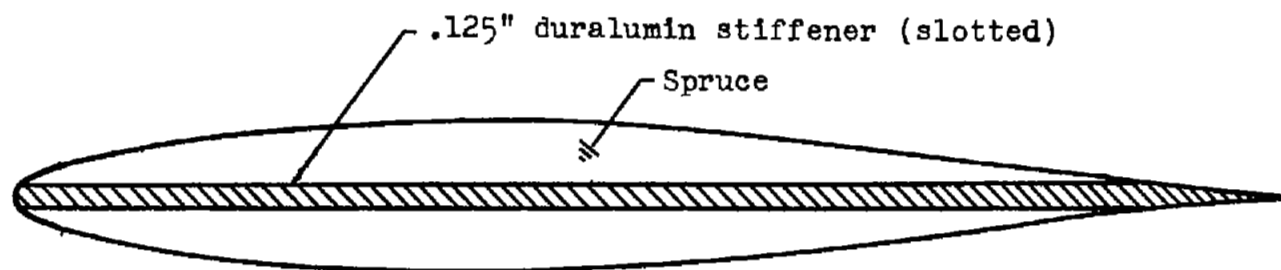
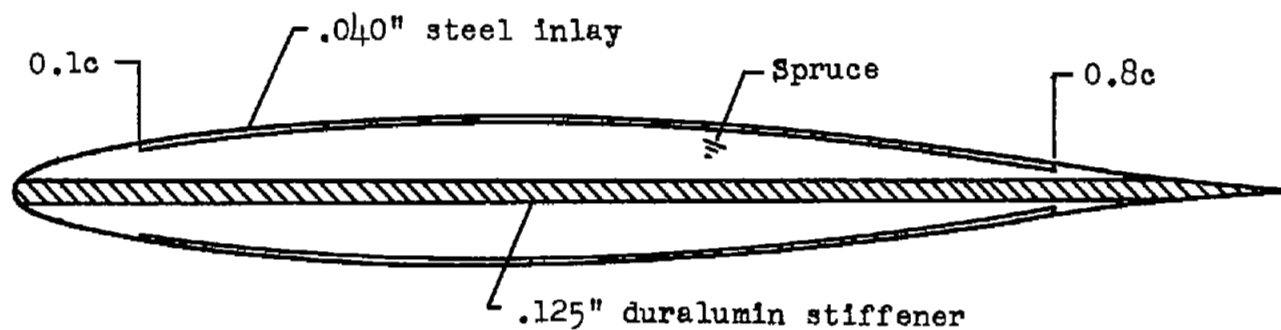


Figure 2.- Geometric details and dimensions of test models.



Models 1 and 3



Models 2 and 4

Figure 3.- Model wing sections in a plane perpendicular to the 38-percent-chord line (drawn to scale).

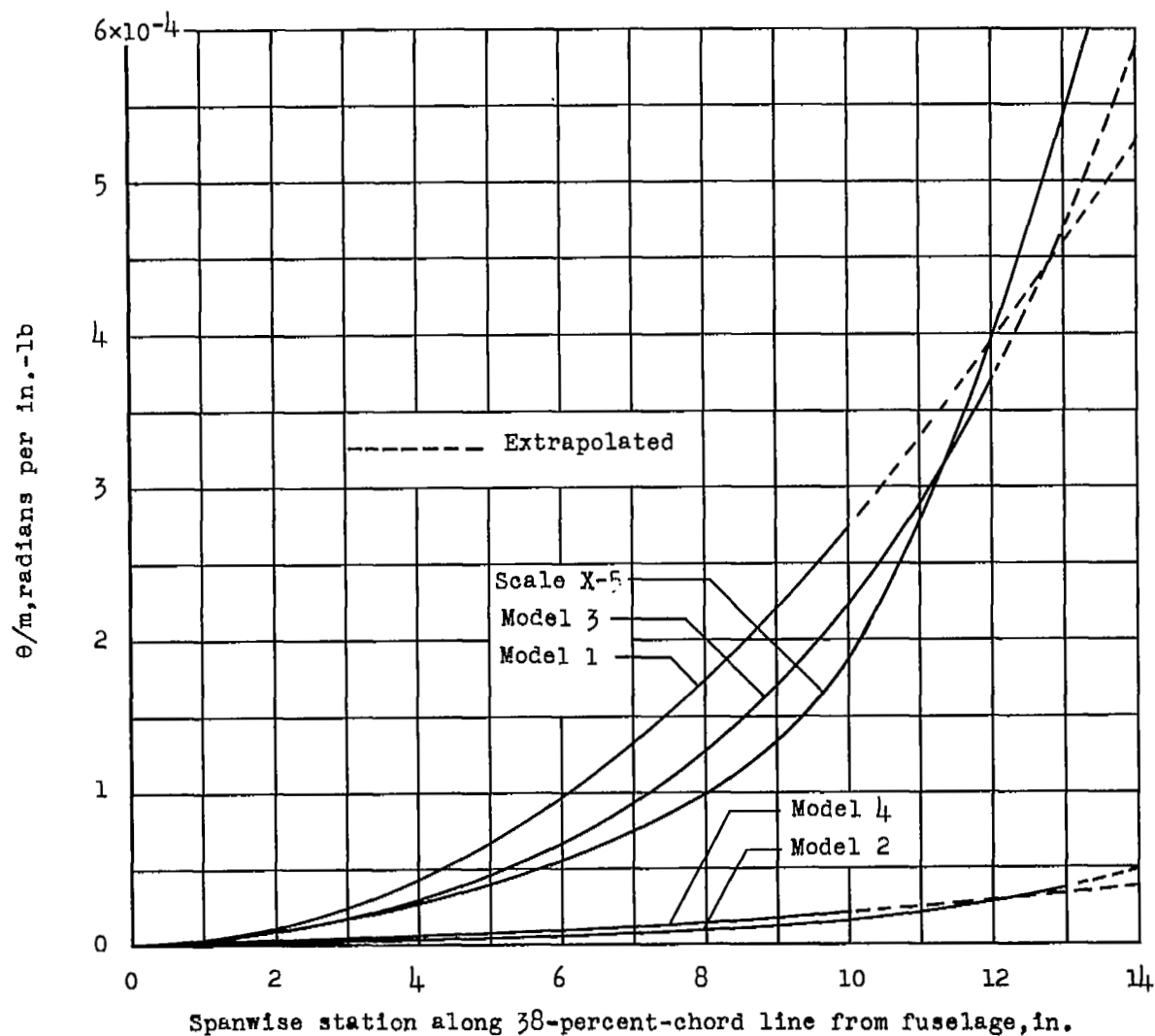


Figure 4.- Spanwise variation of torsional-stiffness parameter θ/m measured in planes perpendicular to the 38-percent-chord line.

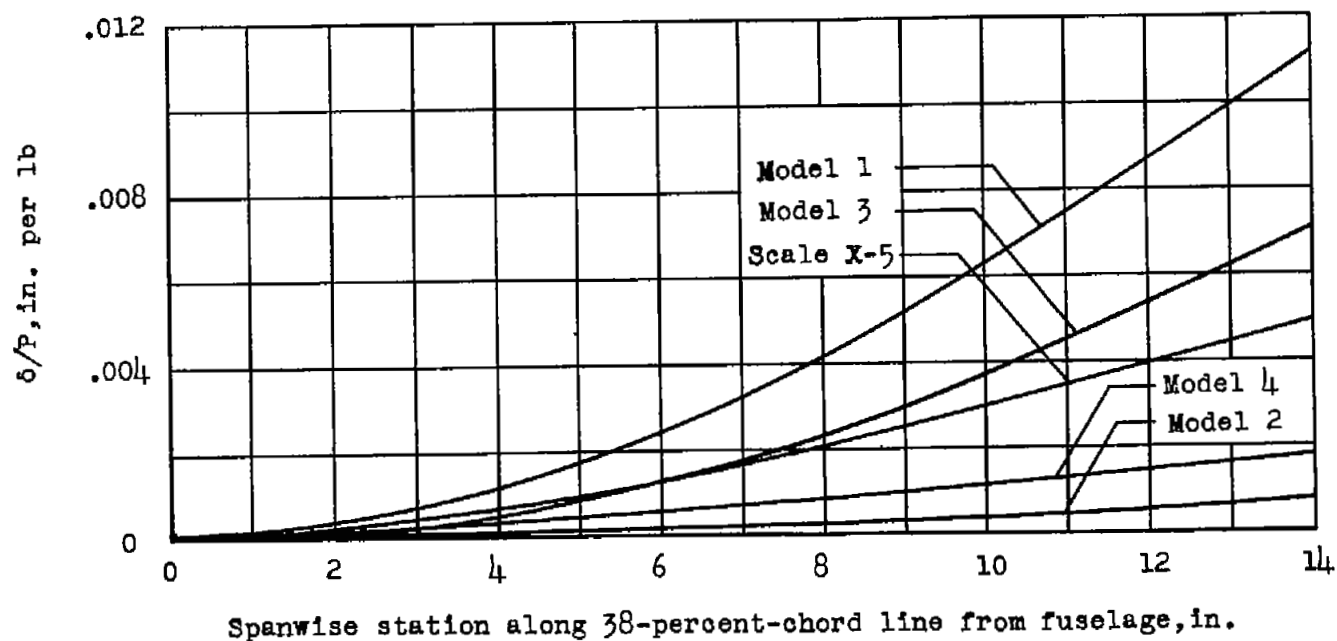
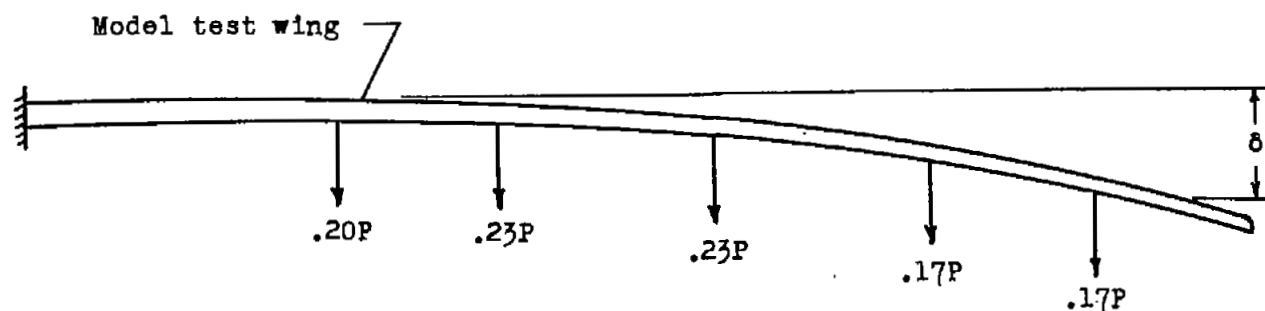


Figure 5.- Spanwise variation of flexural-stiffness parameter δ/P measured along the 38-percent-chord line.

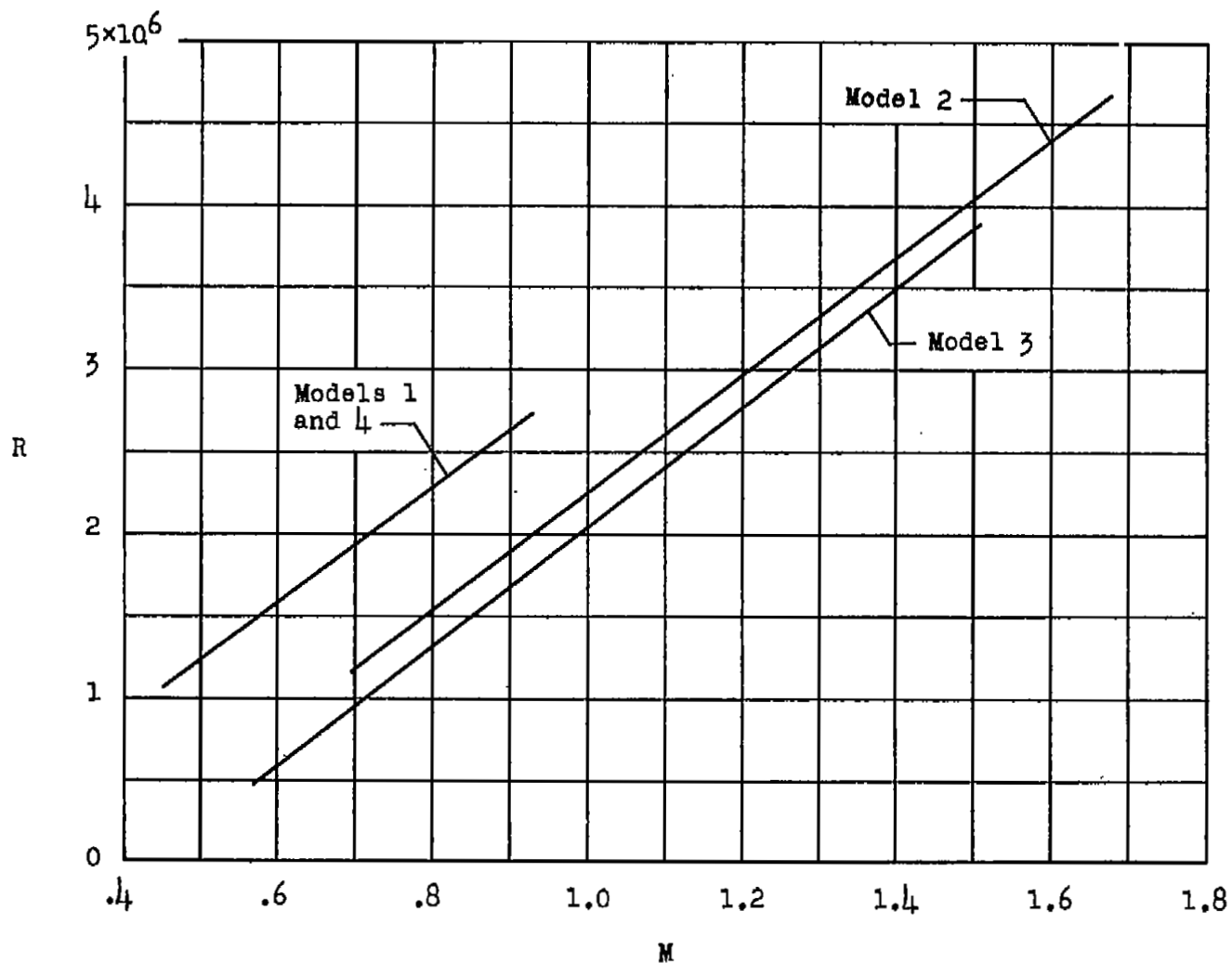


Figure 6.- Range of test Reynolds number plotted against Mach number.
Reynolds numbers based on mean exposed chord of unswept wing panel
(0.445 foot).

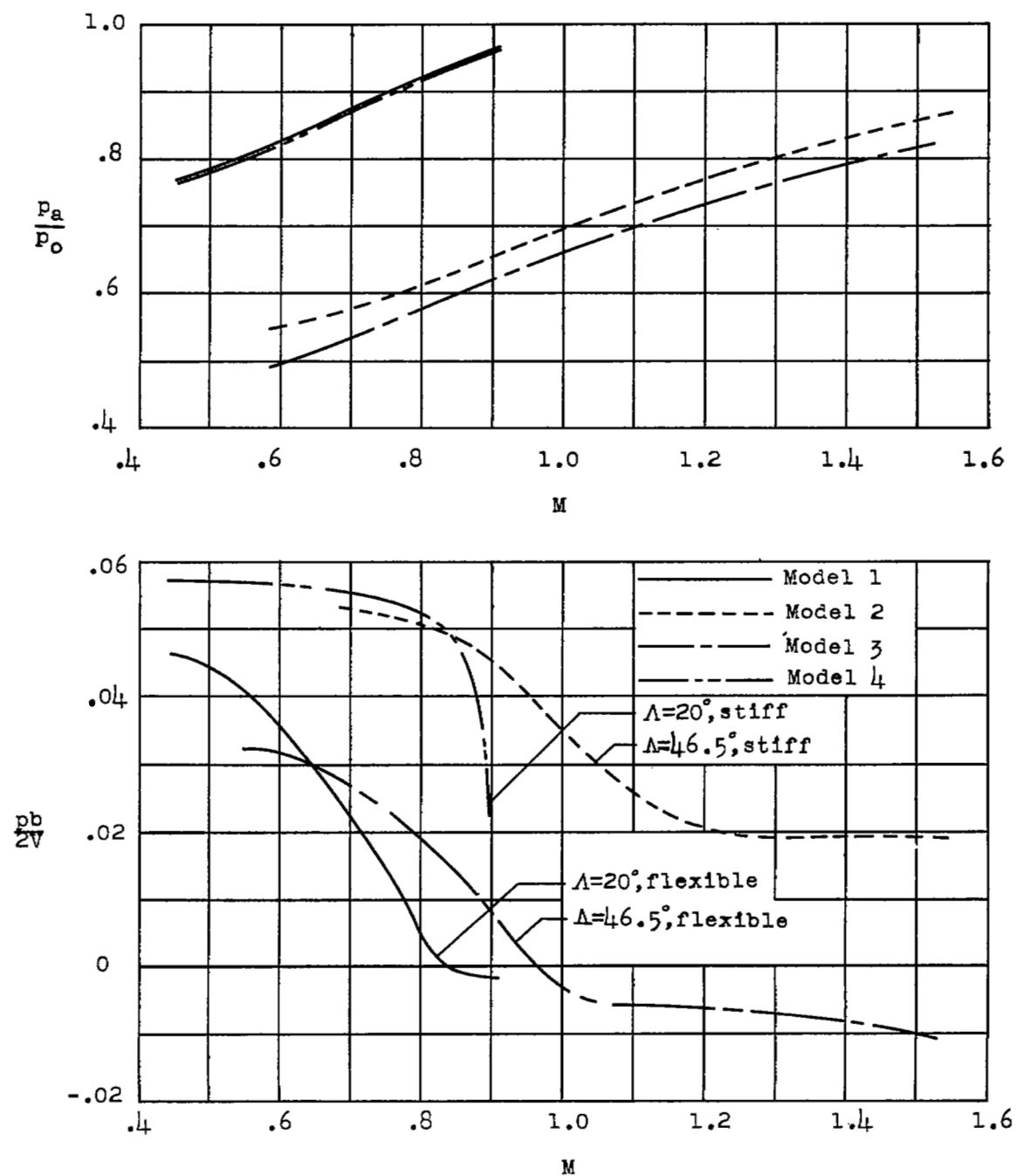
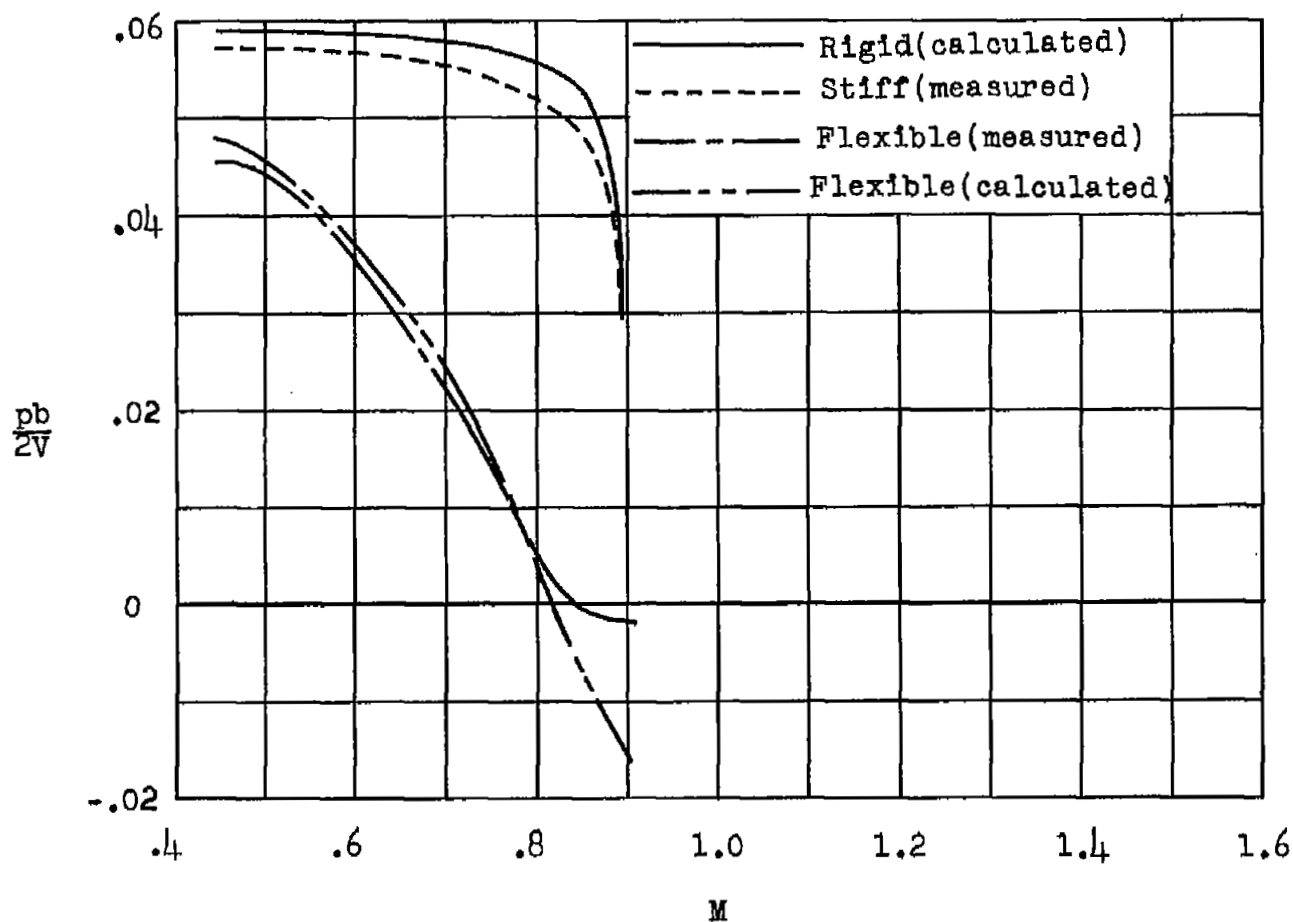
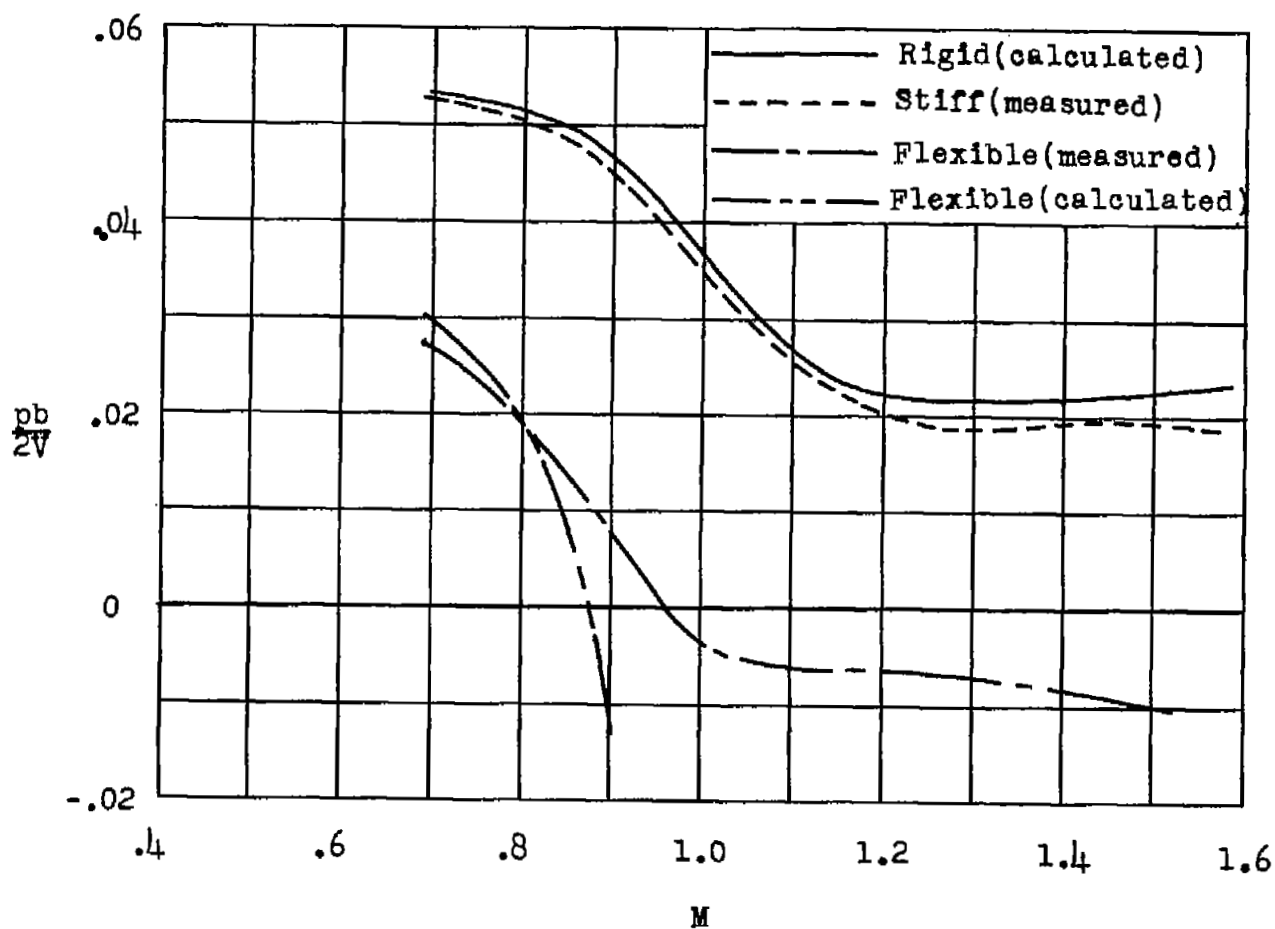


Figure 7.- Variation of p_a/p_o and rolling effectiveness parameter $pb/2V$ with Mach number for all models. $\alpha = 0^\circ$; $\beta = 0^\circ$; $\delta_{a_T} = 20^\circ$.



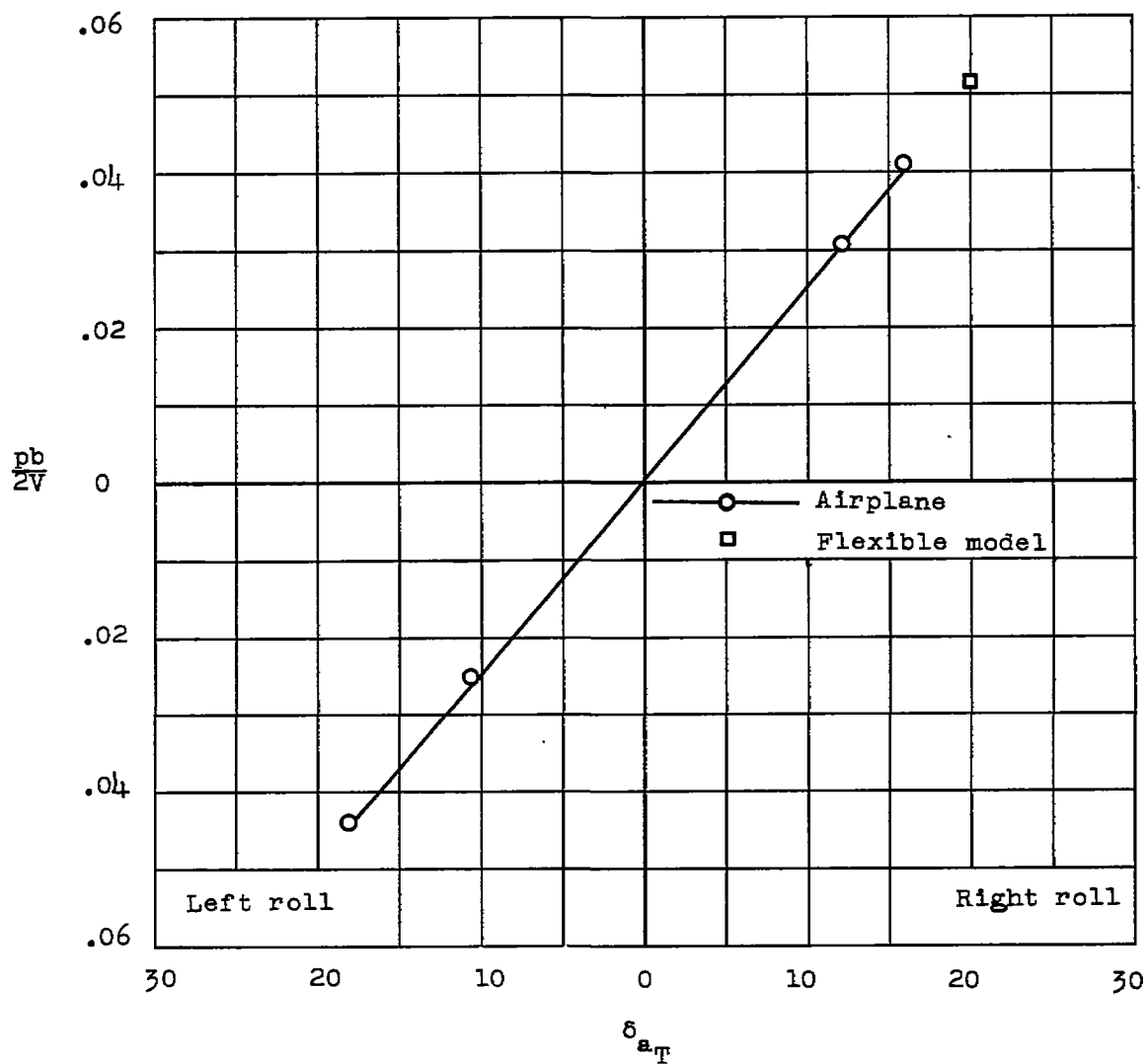
(a) $\Lambda = 20^\circ$.

Figure 8.- Comparison of calculated rigid and flexible rolling effectiveness with measured stiff and flexible rolling effectiveness at test altitudes. $\alpha = 0^\circ$; $\beta = 0^\circ$; $\delta_{a_{II}} = 20^\circ$.



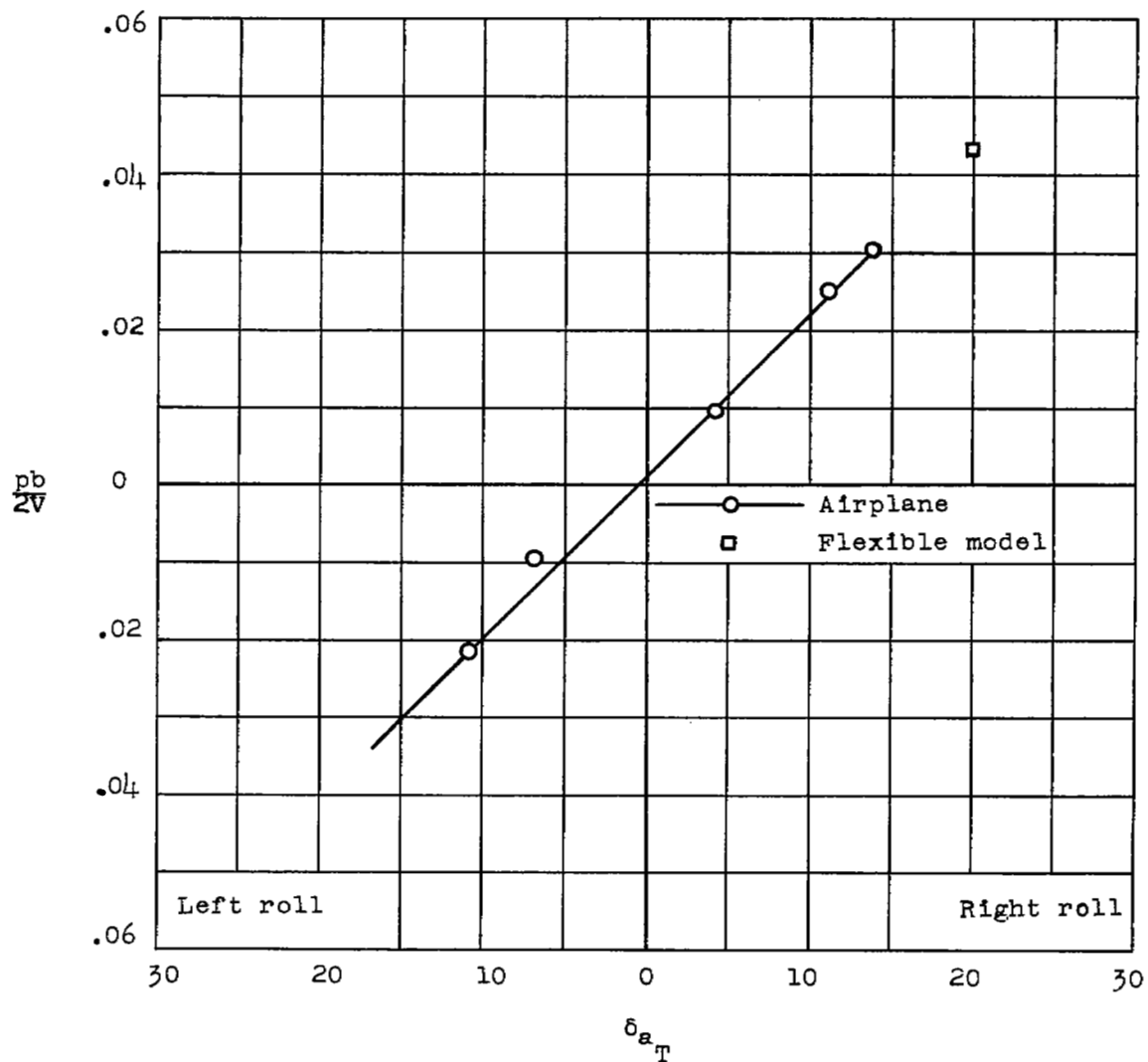
(b) $\Lambda = 46.5^\circ$.

Figure 8.- Concluded.



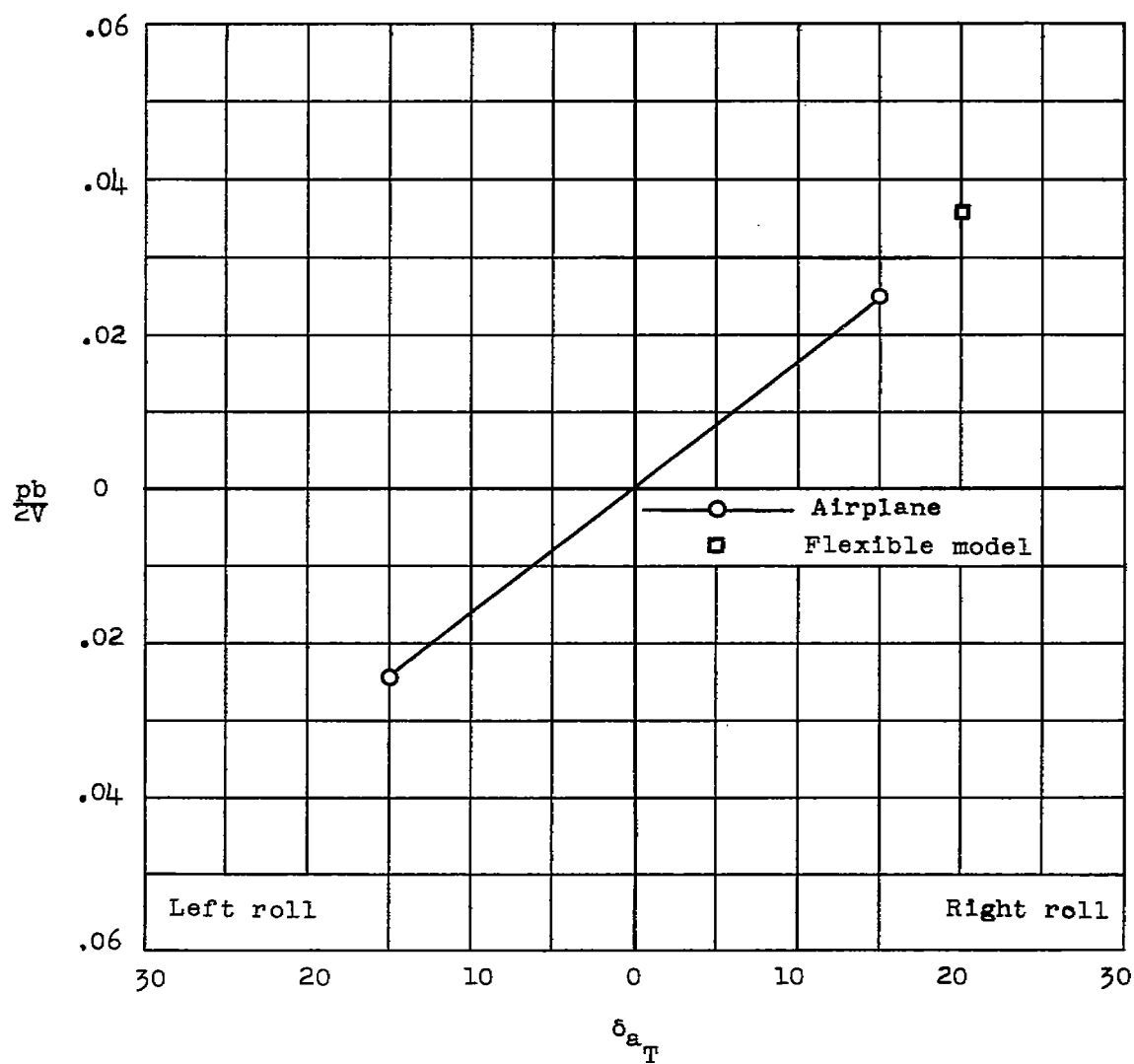
(a) $M = 0.54$.

Figure 9.- Variation of rolling effectiveness parameter $\frac{pb}{2V}$ with total aileron deflection. $\Lambda = 20^\circ$; $h \approx 25,000$ feet; $\beta = 0^\circ$.



(b) $M = 0.72$.

Figure 9.- Continued.



(c) $M = 0.81$.

Figure 9.- Concluded.

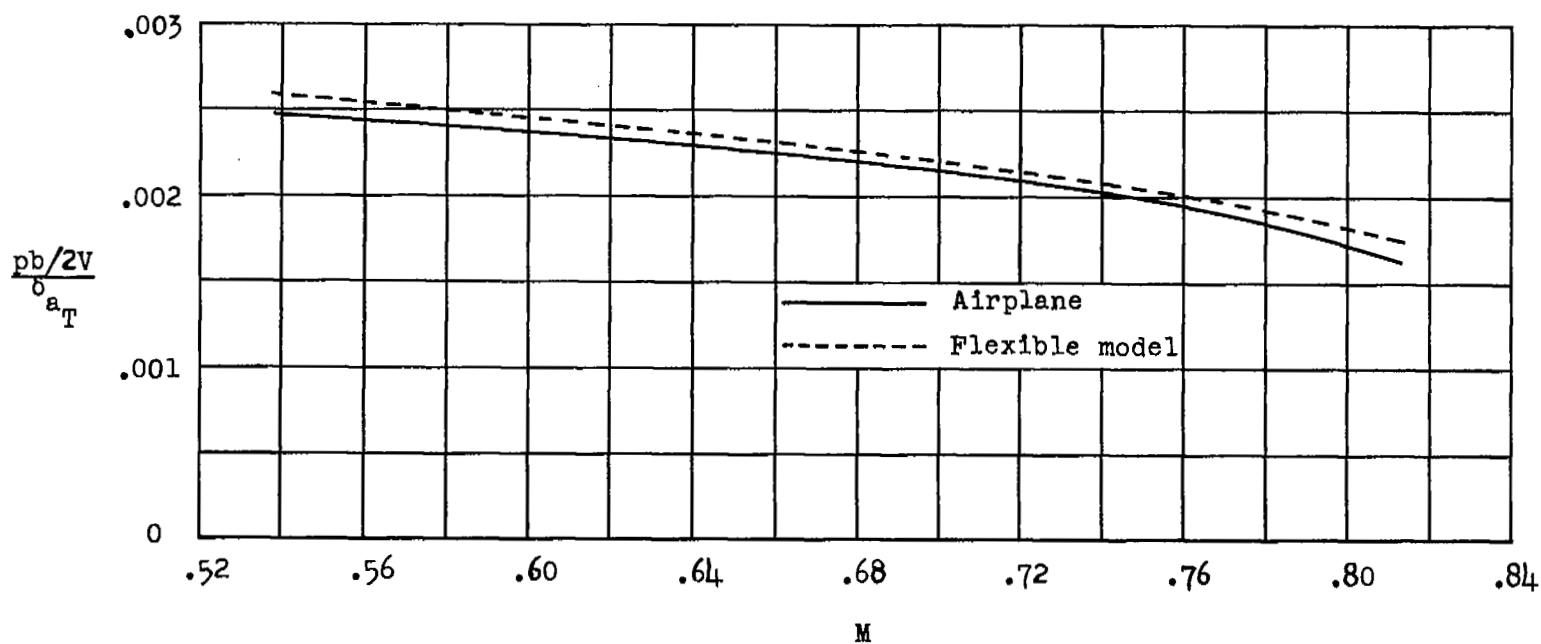


Figure 10.- Variation of rolling effectiveness per degree of total aileron deflection with Mach number. $\Lambda = 20^\circ$; $h \approx 25,000$ feet.

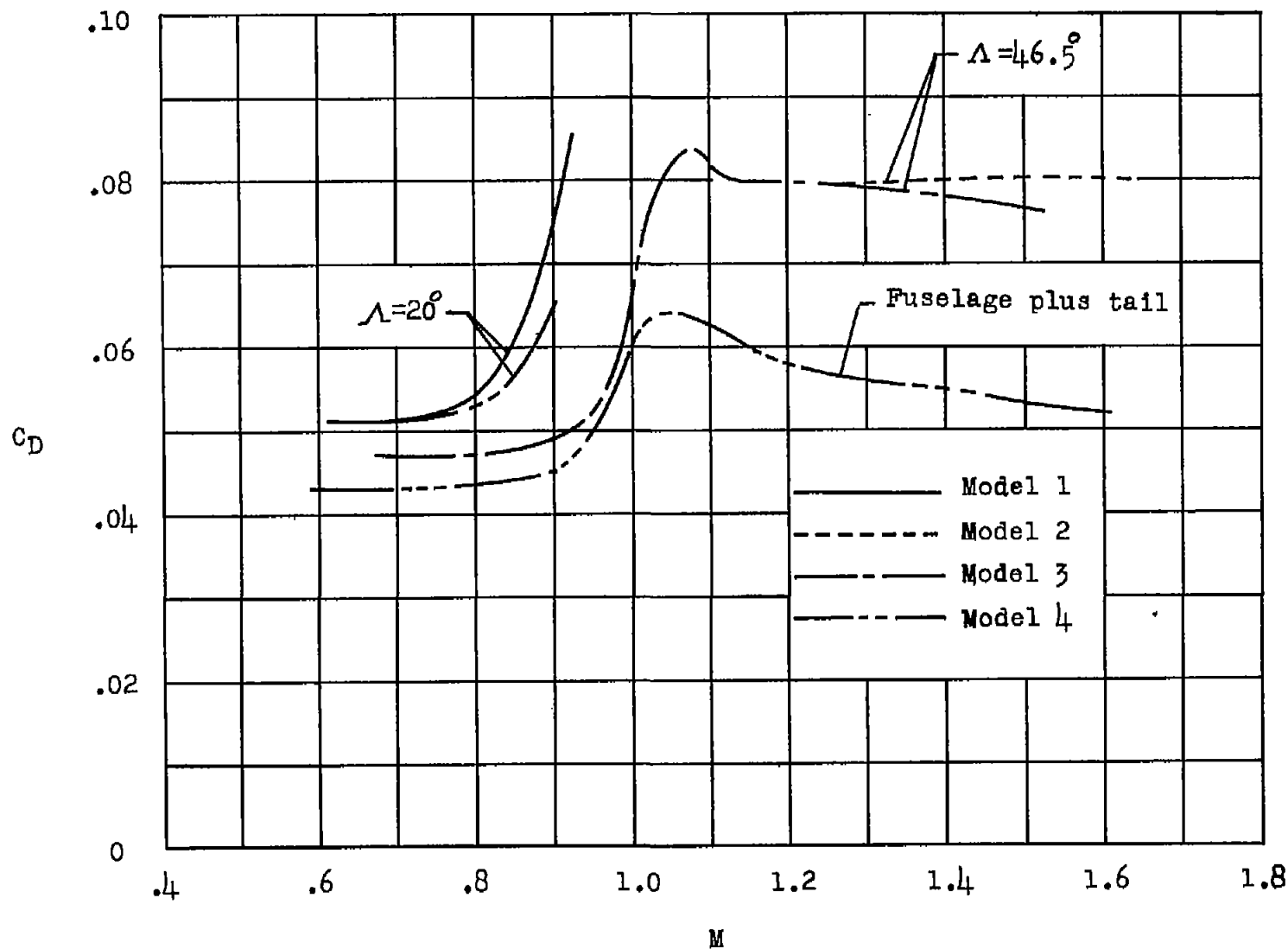


Figure 11.- Variation of drag coefficient C_D with Mach number.

SECURITY INFORMATION

NASA Technical Library



3 1176 01438 0209

[REDACTED]